

Characterization of primary dendrite morphology in complex shaped lamellar cast iron castings

P. Svidró^{1*}, L. Elmquist², I. Dugic³ and A. Diószegi¹

¹Department of Materials and Manufacturing - Foundry Technology, Jönköping University, Jönköping, Sweden

²SinterCast AB, Katrineholm, Sweden

³Department of Mechanical Engineering, Linnaeus University, Växjö, Sweden

Shrinkage porosity and metal expansion penetration are two fundamental defects appearing during the production of complex shaped lamellar cast iron components. Simplified test models simulating the thermal and geometrical conditions existing in complex shaped castings have been successfully used to provoke shrinkage porosity and metal expansion penetration. A stereological investigation of the primary dendrite morphology indicates a maximum intra-dendritic space in connection with the casting surface where the porosity and the penetration defects appear. Away from the defect formation area the intra-dendritic space decreases. Comparison of the simulated local solidification times and measured intra-dendritic space indicates a strong relation which can be explained by the dynamic ripening process. The slow local solidification time situated at the boundary between the casting surface and its surrounding is explained to be the reason for the formation of an austenite morphology which can promote mass flow between dendrites, thereby provoking shrinkage porosity or metal expansion penetration.

Keywords: lamellar cast iron, primary austenite, dendrite morphology, coarsening, shrinkage porosity, metal expansion penetration.

Introduction

Complex shaped lamellar cast iron castings are the most widespread application of cast iron materials. The automotive industry is the largest consumer of this type of cast component. Despite the advantages of good thermal conductivity, high damping capacity and good machinability, some recurrent defects like shrinkage porosity (SP) and metal expansion penetration (MEP) create additional expense for the casting producers and users. Shrinkage porosity can cause leakage through the casting wall when the component is pressurized. Metal expansion penetration can require additional and unhealthy cleaning procedures leading to “white fingers”, an occupational disease. Great efforts have been made to investigate the mechanism of defect formation and to reduce the number of reject castings due to SP and MEP. Metal expansion penetration has been investigated in detail by Levelink et al^{1,2} where they determined that liquid metal was squeezed out from the casting volume and forced between the molding sand grains and causing the defect. They attributed the driving force for MEP formation as the presence of phosphorus and late solidification of the phosphorus eutectic, hence the time for penetration was assumed to be the end of solidification. Later, Dugic et al³ demonstrated that the time for penetration was in fact the beginning of the eutectic phase formation. Dugic and co-workers used non-welded thermocouples to detect when the liquid metal entered the penetrated zone. Formation of shrinkage porosity in foundry practice was believed to take place at the end of the solidification, which was a quite unreasonable statement because lamellar cast iron precipitates low density graphite during the late stage of solidification, providing a liquid surplus that should compensate for the liquid-to-solid contraction. The statements were based on the observation of porosity between the eutectic colonies in the last solidifying areas, with the porosity located between dendrite arms.

An important tool for investigation of SP and MEP was created when techniques for color etching⁴ and Direct Austempering After Solidification (DAAS)^{5,6} were introduced into cast iron research. Diószegi et al^{7,8}, using color etching revealed and distinguished a perfect eutectic composition or an intra-dendritic alloy in the penetrated layers between the sand grains while the original composition of the cast iron was a standard hypoeutectic alloy with minor addition of pearlite stabilizer elements. This was the first observation to show the presence of primary austenite grains and a flow path related to austenite grains observed on the DAAS treated samples. Elmquist et al⁹, used the same method of color etching on samples showing SP. In the color etched samples it became clear that shrinkage porosity did not surround single eutectic colonies, but instead several groups of cells. Further investigation¹⁰ based on DAAS revealed that shrinkage porosity was located at austenite grain boundaries. Later investigation¹¹ based on Electron Back Scattering Diffraction (EBSD) confirmed the locations of the pores at the grain boundaries. The internal surface of the

* Corresponding author, email: peter.svidro@jth.hj.se

shrinkage porosity was found to be oxidized, suggesting a connection to the surrounding atmosphere. Oxidizing gases from the surrounding atmosphere were assumed to flow into the intra-granular area, a material transport path opposite to the one observed during MEP.

Advances in characterization of the primary dendrite morphology¹² and recent demonstration of the dendrite coarsening phenomena during solidification of hypoeutectic lamellar cast iron^{13, 14} motivates the present work, which aims to characterize the liquid flow paths during the formation of MEP and SP as a mean to clarify the mechanics of formation of these defects.

Experimental Procedure

The aim of the experiment is to carry out a quantitative analysis of the primary austenite morphology in regions affected by shrinkage porosity and metal expansion penetration. Samples taken from test castings previously developed to reproduce the thermal conditions in complex shaped castings, and showing the relevant casting defects were used. The casting alloy was hypoeutectic grey cast iron of similar composition to alloys used in the commercial production of automotive cast iron components.

Shrinkage porosity

A casting sample, here “Sample A”, combining simple geometrical domains of cylinders and plates according to Fig. 1 was used¹⁰ to create thermal fields comparable to those found in complex shaped cylinder heads. The chosen geometry is prone to form shrinkage porosity similar to that found in real castings. A lamellar cast iron alloy used in an industrial foundry process, with the composition presented in Table 1, melted in an induction furnace and treated according to the current production procedure was cast into a mold prepared using Epoxi-SO₂ hardened quartz sand. Sample A was cut as indicated by the dashed lines in Fig. 1. The cut surface including the lower cross section of the middle cylindrical domain (Fig. 2) shows shrinkage porosity of the same type as it is described in the literature⁹, namely the porosity is formed in connection with the casting surface, and forms between eutectic colonies where primary austenite dendrites can be observed (Fig. 3).

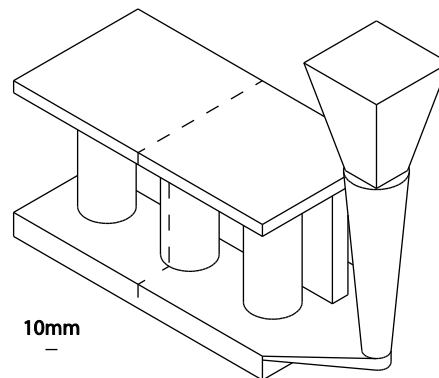


Fig.1: Sample A, combines a 10 mm top plate and a 20 mm bottom plate interconnected with three cylinders (\varnothing 40 mm) and a wall of 15 mm parallel to the cylinders. The minimum distance between the vertical plate and the cylinder is 7 mm.

Table 1: Chemical composition of Sample A.

Element	C [%]	Si [%]	Mn [%]	P [%]	S [%]	Cr [%]	Mo [%]
Sample A	3.28	1.96	0.64	0.03	0.06	0.26	0.05

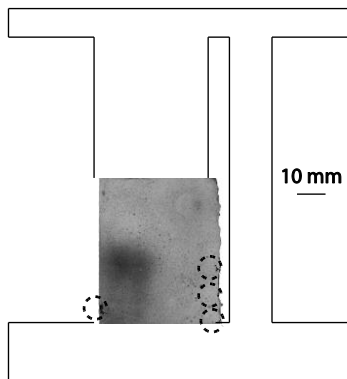


Fig.2: Sample A, investigated cross section. Circles of dashed lines indicate where shrinkage porosity connected to the casting surface was observed.

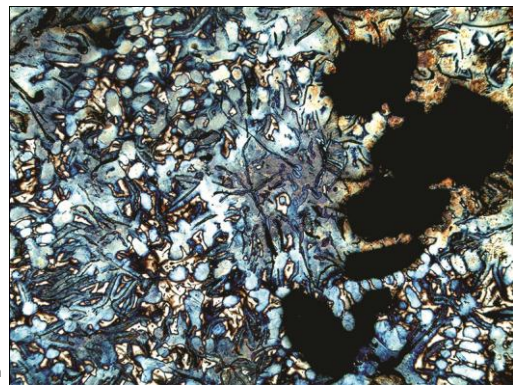


Fig.3: Sample A, color etched micrograph from the investigated cross section showing SP.

Metal Expansion Penetration

The casting sample used here “Sample B”, is a combination of a cylindrical casting with diameter Ø80 mm x 80 mm tall with an internal cylindrical channel with Ø30 mm and an internal concave casting surface with R15 mm. The cross section of the mold used to produce Sample B is shown in Fig. 4, is identical with that discussed in the literature^{7, 8} and is designed to promote metal expansion penetration. Similar molding materials and liquid metal from the same foundry process were used as for “Sample A” except for the chemical composition which is shown in Table 2.

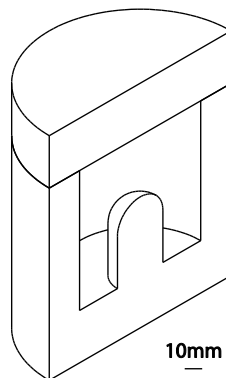


Fig.4: Sample B, a half section of the mold.

Table 2: Chemical composition of Sample B.

Element	C [%]	Si [%]	Mn [%]	P [%]	S [%]	Cr [%]	Mo [%]
Sample A	3.18	1.77	0.56	0.05	0.09	0.15	0.24

The Sample B casting was cut in half and prepared for metallographic observation as shown in Fig. 5. Sample B is rotational-symmetric and penetration defects appeared evenly distributed across the internal concave casting surface as marked on Fig 5. The exuded metal which penetrates the mold appears to contain a perfect eutectic composition as shown in the left lower corner of Fig. 6. The chemical composition (Table 2) is a hypoeutectic alloy, which implies that primary austenite should form under stable solidification conditions. The microstructure of the bulk material belonging to the sample connected to the concave casting surface (upper right corner of Figure 6) contains primary austenite dendrites (highlighted with red color) between the eutectic colonies. This is the evidence that the metal present in the region has solidified according to the stable solidification condition. The material in the lower left part of Fig. 5 is the penetrated material behind the casting surface and contains only individual graphite flakes embedded in the metallic matrix without any evidence of primary austenite dendrites. This particular combination was mentioned in the introduction to be previously discussed in the literature as indicating that the intra-dendritic liquid in the bulk material of the sample after the formation of the primary austenite dendrite and segregation up to a close eutectic composition has been forced into the interstices between the sand grains of the mold.

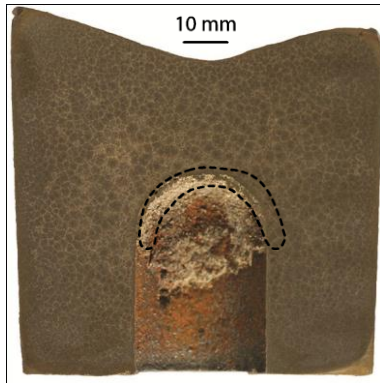


Fig.5: Sample B, a cross section of a cylindrical casting sample, dashed line indicates the penetrated area.

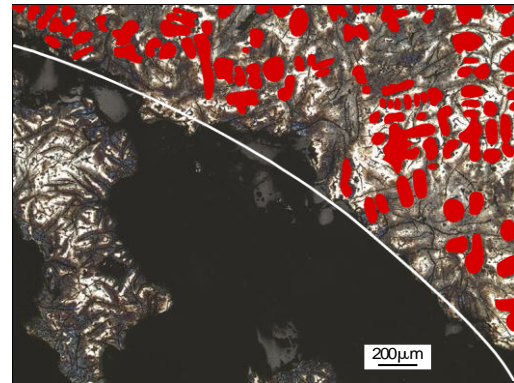


Fig.6: Sample B, a color-etched micrograph showing the microstructure in the penetrated zone. The upper right corner belongs to the casting while the lower left corner represents the penetrated metallic matrix.
Red – primary austenite dendrites.
White line is the mold-metal interface.

Image analysis and stereological definitions

The surfaces of samples A and B were color-etched using the standard picric acid-based technique⁴ at elevated temperature. Characterization of the microstructure components has improved since digital image analysis has been introduced, which allows a more sophisticated examination of the morphology. In the case of cast iron the use of color etching in combination with image analysis opened up the characterization potential of the primary austenite network. The color distribution obtained by picric acid-based etching is strictly dependent on the silicon segregation pattern¹⁵.

Positive segregation of Si ($k > 1$) creates a well distinguished picture of the primary austenite only where the primary network is not superimposed on the eutectic colony. As a consequence it is necessary to consider the equal distribution of the primary austenite in the casting domain. For this reason a distinguishing procedure has been adapted by dividing the investigated area into clear primary austenite, clear intra-dendritic space and not distinguishable areas. The procedure is presented in Fig. 7 and Fig. 8. Fig. 7 shows the color-etched microstructure including the entire dendritic austenite network and the superimposed eutectic cells. Fig. 8 shows the pre-processed structure performed in combination between image analysis software and a manual touch-pad screen.

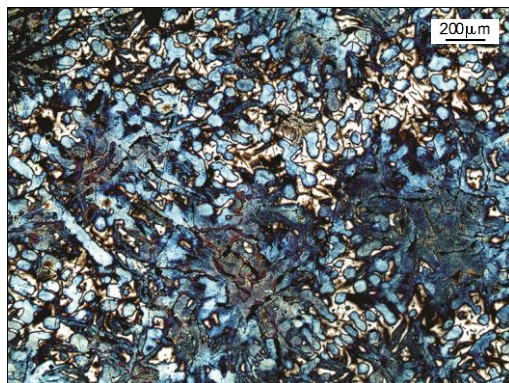


Fig.7: A color-etched micrograph from Sample A.



Fig.8: Pre-processed structure for image analysis.
Red – primary austenite
Black – intra-dendritic space
Green – excluded from the measurement, as it is obscure.

Three units showing primary austenite dendrites were investigated. Secondary dendrite arm spacing (SDAS) given in mm was measured as well the surface area A_i of the intra-dendritic phase and the perimeter P_i between the observed primary austenite phase and the intra-dendritic space. Recent research work¹² demonstrated a stereological parameter useful for the present research work to characterize the local intra-dendritic space as a measure to indicate the flow path direction during formation of MEP and SP. This parameter was called the *modulus of the intra-dendritic phase*, M_{IP} and relates the volumes of the intra-dendritic phase and its envelope. Invocation of stereological rules demonstrated that M_{IP} as a 3-D parameter can be approximated by comparing A_i and P_i obtained from a 2-D planar observation. The modulus of the intra-dendritic space is comparable with the hydraulic diameter used in fluid dynamics $M_{IP} = \frac{A_i}{P_i}$ with a unit of μm . Recent research^{13, 14} in the field of lamellar cast iron solidification demonstrated the occurrence of dynamic

Experimental results and discussion

Solidification results in both cases presented in Fig. 9 and Fig. 10 indicate that the longest local solidification times are found at the casting-mold boundary where MEP and SP are formed in real castings. The same tendency can be observed for the calculated modulus of intra-dendritic space where the largest interspaces correspond to the longest simulated local solidification times. Based on the calculated local solidification time it can be concluded that the largest intra-dendritic space in the casting is situated at the casting-mold boundary and decreases continuously as the local solidification time decreases. The gradient in M_{IP} is also an indication of how the inter-dendritic melt existing during solidification of the lamellar cast iron can serve as a transport path to the surroundings. This path can transport material in both directions as is described in the literature, from the surroundings into the casting as in the case of shrinkage compensation and inversely from the inner domains of the casting to the surrounding as in the case of metal expansion penetration.

Fig. 11 and Fig. 12 compare both the modulus of the intra-dendritic phase M_{IP} and the secondary dendrite arm spacing SDAS to the calculated local solidification time with literature data¹⁶ obtained in previous work. The literature results were obtained as the average on cylindrical samples ($\varnothing 40\text{mm} \times 40\text{mm}$) cast separately from the same raw material at different cooling rates. In the present work the results were collected from the complex shaped samples A and B where the different cooling rates were created within the same sample.

Comparing the morphological parameters M_{IP} seems to give less scatter in the result than SDAS for both solidification cases in samples A and B. Apart from the influence of the local solidification time, which was calculated without taking into account the ripening phenomena - the differences in the scatter can be attributed to fragmentation of the dendritic network, which is reported in the literature¹⁷. Dendrite fragmentation is an obstacle to accurate SDAS measurement.

The relatively good correlations for both M_{IP} and SDAS with respect to the literature data presented in Figure 11 and Figure 12 are remarkable because the values from the literature were demonstrated to depend strictly on the coarsening process of the dendritic network during the columnar to equiaxed transition and the end of the solidification.

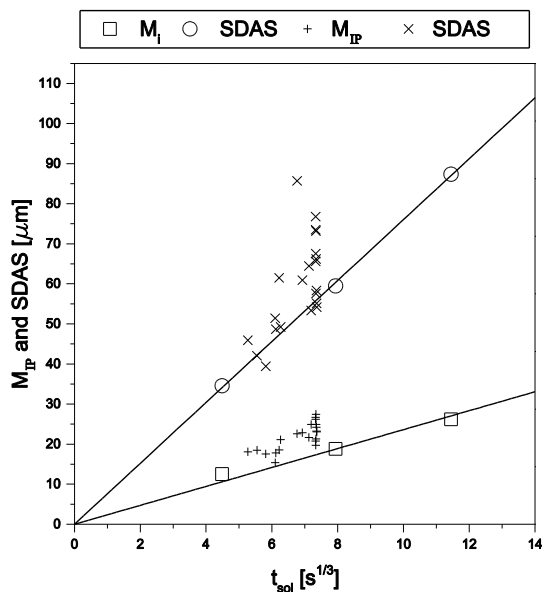


Fig.11: Measured SDAS and M_{IP} as a function of time compared to the literature data in sample A.

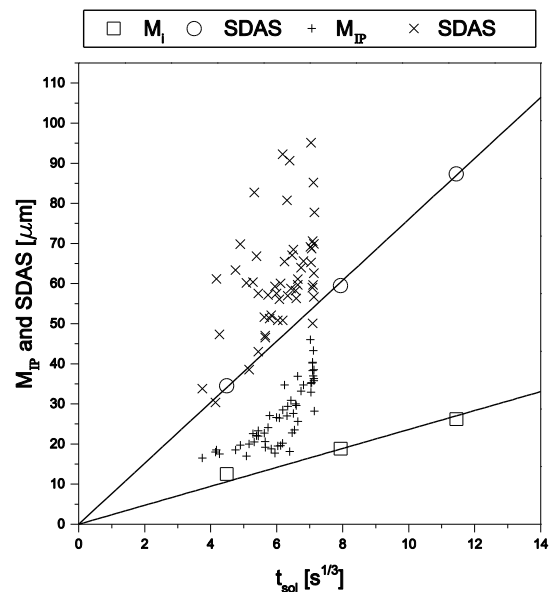


Fig.12: Measured SDAS and M_{IP} as a function of time compared to the literature data in sample B.

Conclusions

1. The local solidification time affects the austenite morphology in complex shaped castings.
2. When the local solidification time (t) increases, the modulus of intra-dendritic space M_{IP} and the secondary dendrite arm space (SDAS) also increase.
3. The increasing value of the modulus of the intra-dendritic phase can be explained by the dynamic coarsening process.
4. The presence of thermal conditions leading to the slowest local solidification time at the boundary between the casting surface and its surroundings cause the formation of an austenite morphology which can promote mass flow between dendrites, thereby provoking shrinkage porosity or metal expansion penetration.

References

1. H. G. Levelink and F. P. M. A. Julien: AFS Cast Met. Res. J., 1973, 9, 2, 56–63.
2. H. G. Levelink and F. P. M. A. Julien: AFS Cast Met. Res. J., 1973, 9, 2, 105–109.
3. I. Dugic and I. L. Svensson: Int. J. Cast Met. Res., 1999, 11, 5, 333–338.
4. A. Diószegi: 'On the microstructure formation and mechanical properties in grey cast iron', PhD thesis, Linköping University, Linköping, Sweden, 2004.
5. G. L. Rivera, R. E. Boeri, and J. A. Sikora: Scr. Mater., 2004, 50, 3, 331–335.
6. G. Rivera, P. Calvillo, R. Boeri, Y. Houbaert, and J. Sikora: Mater. Charact., 2008, 59, 9, 1342–1348.
7. A. Diószegi and I. Dugic: Proc. 'Science and Processing of Cast Iron VIII', Beijing, China, October 2006. 92-97.
8. A. Diószegi, I. Dugic, and I. L. Svensson: AFS Trans., 2007, 115, 609–615.
9. L. Elmquist, S. Adolfsson, and A. Diószegi: Proc. '112th Metalcasting Congress', Atlanta, GA, USA, May 2008, Paper 08-105(05).
10. L. Elmquist and A. Diószegi: Int. J. Cast Met. Res., 2010, 23, 1, 44–50.
11. L. Elmquist, K. Soivio, and A. Diószegi: Mater. Sci. Forum, 2014, 790–791, 441–446.
12. A. Diószegi, V. Fourlakidis, and R. Lora: Proc. '10th International Symposium on the Science and Processing of Cast Iron', Mar Del Plata, Argentina, September 2014.
13. A. Diószegi, R. Lora, and V. Fourlakidis: Mater. Sci. Forum, 2014, 790–791, 205–210.
14. V. Fourlakidis, R. Lora, and A. Diószegi: Mater. Sci. Forum, 2014, 790–791, 211–216.
15. S. Vazehrad, J. Elfsberg, and A. Diószegi: Int. J. Mater. Charact., 2014.
16. R. Lora and A. Diószegi: Metall. Mater. Trans. A, 2012, 43, 13, 5165–5172.
17. J. C. Hernando: 'Isothermal coarsening of primary austenite in Lamellar Cast Iron', Master thesis, Jönköping University, Jönköping, 2013.

Acknowledgements

The present work is a part of the research project JÄRNKOLL within the Casting Innovation Centre, financed by the Swedish Knowledge Foundation. Cooperating parties in the project are Jönköping University, Swerea SWECAST AB, Scania CV AB and Volvo Powertrain AB. Participating persons from these institutions/companies are acknowledged.